Paper No.
10997

NACE INTERNATIONAL CORROSION 2018 Conference & Expo

Effect of Alloying Elements on the Corrosion Behavior of Carbon Steel in CO_2 Environments

Yoon-Seok Choi, Srdjan Nesic
Institute for Corrosion and Multiphase Technology,
Department of Chemical and Biomolecular Engineering, Ohio University
342 West State Street
Athens, OH 45701
USA

Hwan-Gyo Jung
Technical Research Lab., POSCO
Pohang, South Korea

ABSTRACT

The objective of the present study was to evaluate the effect of alloying elements (Cr, Mo and Cu) on the corrosion behavior of low carbon steel in CO_2 environments. Six samples were prepared with varying Cr content from 0 to 2 wt.% and with added 0.5 wt.% of Mo and Cu; the specimens had ferritic/pearlitic microstructures. Steel samples were exposed to a CO_2-saturated 1 wt.% NaCl solution with different combinations of pH and temperature (pH 4.0 at 25°C, pH 6.6 at 80°C, and pH 5.9 at 70°C). Changes in corrosion rate with time were determined by linear polarization resistance (LPR) measurements. The surface morphology and the composition of the corrosion product layers were analyzed by surface analysis techniques (SEM and EDS). Results showed that the addition of Cr and Cu showed a slight positive effect on the corrosion resistance at pH 4.0 and 25°C. At pH 6.6 and 80°C, regardless of the alloying elements, the trend of corrosion rate with time was similar, *i.e.*, the corrosion rate of all specimens decreased with time due to the formation of protective $FeCO_3$. A beneficial effect of Cr addition was clearly seen at pH 5.9 and 70°C, where steel sample without Cr showed no decrease in corrosion rate with time. The addition of Cr promotes the formation of protective $FeCO_3$ and it decreases the corrosion rate.

Key words: CO_2 corrosion, carbon steel, alloying element, $FeCO_3$

INTRODUCTION

Internal environments encountered in the oil and gas transportation pipelines can cause severe corrosion of mild steel mainly due to the presence of CO_2, H_2S, organic acids, and water. In CO_2 environments, low carbon steel has often been used in combination with corrosion inhibitor since it is considered the most cost effective option, compared with utilizing expensive Corrosion Resistance Alloys (CRA).[1] The corrosion protection of low carbon steel depends on either the spontaneous formation of protective

corrosion product layers which is influenced by environmental parameters (CO_2 content, solution chemistry, pH, temperature, fluid velocity, etc.) and material parameters (microstructure and chemical composition)[2] or the addition of corrosion inhibitors. To date, many studies[3-8] have been conducted to understand the effect of both the environmental and metallurgical conditions on corrosion behavior of steels in CO_2 environments.

In recent years, there has been an attempt to use low-Cr alloy steel (0.5% ~ 3% Cr) in CO_2 environments without inhibitor injection since adding Cr to low alloy steel could enhance corrosion resistance at high temperatures and high pressures.[9,10] It has been reported that the addition of Cr contributes to the enrichment of Cr in the corrosion products, which causes the corrosion product layers to be more protective. In addition, an increase in Cr content could lower both the uniform corrosion rate and susceptibility to localized corrosion in CO_2 environments.[11-16]

Although it is evident that small contents of Cr in low alloy steel decrease the corrosion attack, most of the research studies have focused on the corrosion behavior in very specific ranges of environmental parameters, such as pH, temperature, CO_2 content, etc.[17] Thus, it is necessary to evaluate the effect of Cr addition on the corrosion behavior of low alloy steel under various scenarios encountered in the internal environments for the oil and gas transport pipelines. The objective of the present study was to evaluate the effect of Cr on the corrosion behavior of low alloy steel under different combinations of pH and temperature. Those combinations result in widely differing conditions with respect to whether protective corrosion product layers would form. The effect of minor additions of Mo and Cu on the corrosion behavior was also investigated.

EXPERIMENTAL PROCEDURE

The test specimens with different alloying elements were prepared using the vacuum arc melting furnace and a pilot plant rolling machine. To rule out microstructural effects, the rolling and cooling process were restricted by high temperature rolling (> 850°C) and air-cooling. Total reduction of finish rolling was 75%. All materials were analyzed for chemical composition using Atomic Emission Spectroscopy (AES). Table 1 shows chemical compositions of the six steels used in the present study.

Table 1
Chemical compositions of materials used in the present study (wt.%, balance Fe).

No.	C	Mn	Si	P	S	Al	Cr	Ni	Mo	Cu
1	0.041	1.39	0.278	0.008	<0.003	0.028	-	0.287	-	-
2	0.038	1.43	0.266	0.009	<0.003	0.019	0.519	0.307	-	-
3	0.043	1.45	0.248	0.009	<0.003	0.023	1.000	0.292	-	-
4	0.042	1.40	0.254	0.008	<0.003	0.022	1.890	0.308	-	-
5	0.040	1.41	0.248	0.008	<0.003	0.024	0.520	0.309	0.53	-
6	0.040	1.38	0.248	0.008	<0.003	0.024	0.497	0.307	-	0.50

The specimens for the corrosion test were machined with two different geometries: cylindrical type with 5 cm^2 exposed area for electrochemical measurements, and rectangular type with a size of 1.27 cm × 1.27 cm × 0.254 cm for surface analysis. The specimens were sequentially ground with 250, 400 then 600-grit silicon carbide (SiC) paper, cleaned with isopropyl alcohol in an ultrasonic bath, and dried.

An aqueous electrolyte was prepared from deionized water with 1 wt.% NaCl. The solution was initially deoxygenated by bubbling CO_2. This procedure assured that the dissolved oxygen levels were kept below 20 ppb. The pH of the solution was adjusted by adding either deoxygenated acid (HCl) or base ($NaHCO_3$) in sufficient quantity to reach the desired pH. Corrosion tests were carried out in a 2L glass cell under atmospheric pressure. The setup consists of a: (1) three-electrode corrosion cell (CE: platinum wire, RE:

Ag/AgCl electrode); (2) hot plate equipped with temperature controller; (3) CO_2 gas supply set; (4) condenser; (5) potentiostat; and (6) pH meter.

The corrosion properties of carbon steels were evaluated by electrochemical techniques (open-circuit potential (OCP), linear polarization resistance (LPR), and potentiodynamic polarization measurements), and surface analytical techniques (scanning electron microscopy (SEM), energy dispersive X-ray spectroscopy (EDS)). LPR measurements were performed within ±10 mV with respect to the corrosion potential with a scan rate of 0.166 mV/s. The potentiodynamic polarization tests were carried out after conducting LPR measurements. The specimen was scanned potentiodynamically at a rate of 0.166 mV/s from the OCP to -1.0V vs. sat. Ag/AgCl. Then the scan was performed in the anodic direction from OCP to -0.45V vs. sat. Ag/AgCl, with a scan rate of 0.166 mV/s. After the experiment, the specimen was used for additional *ex-situ* analyses. The morphology and compositions of corrosion products were analyzed by using SEM and EDS.

Table 2 lists the key test conditions for the present study. The test conditions were set in order to investigate the effect of alloying elements for different scenarios common in CO_2 corrosion of mild steel, some of which would include formation of protective $FeCO_3$ corrosion product layers (at high temperature, 80°C) and others would not (at room temperature, 25°C) , with conditions at 70°C being in between.

Table 2
Test conditions for corrosion testing

Condition	pCO_2 (bar)	Temperature (°C)	pH	Solution
$FeCO_3$-free	0.97	25	4	1 wt.% NaCl (stagnant)
$FeCO_3$-forming	0.52	80	6.6	1 wt.% NaCl (stagnant)
In between	0.68	70	5.9	1 wt.% NaCl (stagnant)

RESULTS AND DISCUSSION

Figure 1 shows the microstructure of low carbon steels with different alloying elements. It was taken at quarter position through thickness in transverse direction. The basic microstructure of all samples is ferrite and pearlite mixture. Although the manufacturing process parameters were all the same, the microstructures such as grain size, band structure, and pearlite portion are slightly different because of the alloying elements. The pearlite portion was increased from 7% to 15% with increasing Cr content. Furthermore, the additions of Cr and Mo increased the grain size of ferrite.

Experiments at pH 4 and 25°C

For these conditions where the formation of protective $FeCO_3$ corrosion product layers was not expected, the results of LPR corrosion rate measurements for different carbon steels are described in Figure 2. The polarization resistance values obtained from LPR were converted to corrosion rates with B value of 26 mV. The alloyed steels exhibited more resistance to corrosion than 0.3Ni steel. The results indicate that the addition of Cr slightly decreases the corrosion rate, while additional Cr content had minimal impact. Furthermore, addition of Mo did not change the corrosion rate, but the corrosion rate was slightly reduced by adding Cu.

Figure 3 illustrates the polarization curves for different carbon steels at pH 4 and 25°C. As shown in Figure 3 (a), with increasing Cr content, both anodic and cathodic reaction rates were slightly reduced, supporting the decrease in the corrosion rate. Furthermore, slight reduction in anodic and cathodic current densities are also observed by adding Mo and Cu.

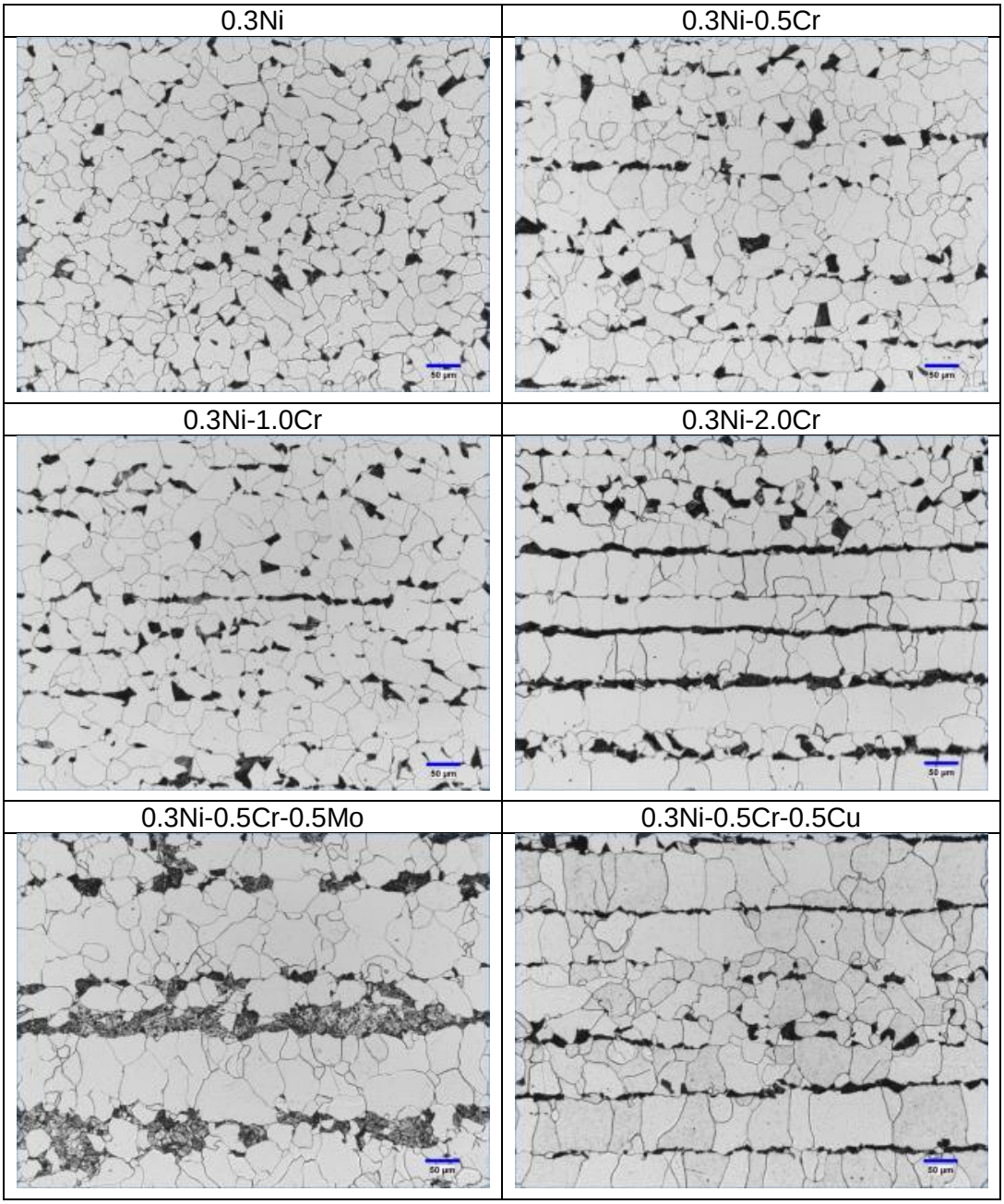

Figure 1: Optical image of the microstructure for different carbon steels (X200, 2% Nital).

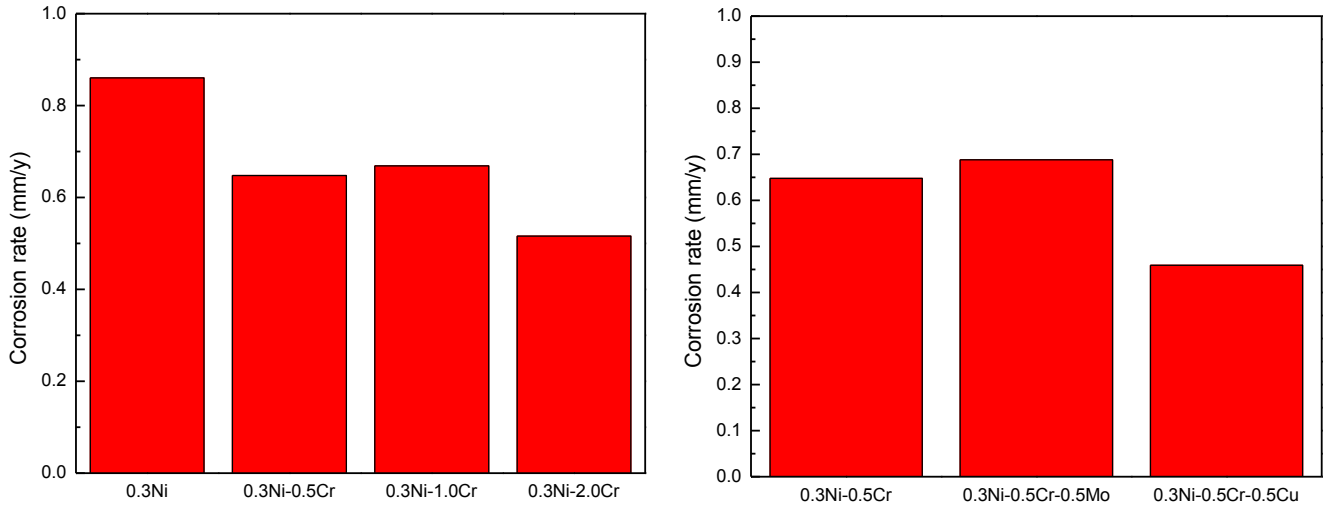

Figure 2: Effect of alloying elements on the corrosion rate in 1 wt.% NaCl solution at pH 4 and 25°C: (a) Cr effect, (b) Mo and Cu effect.

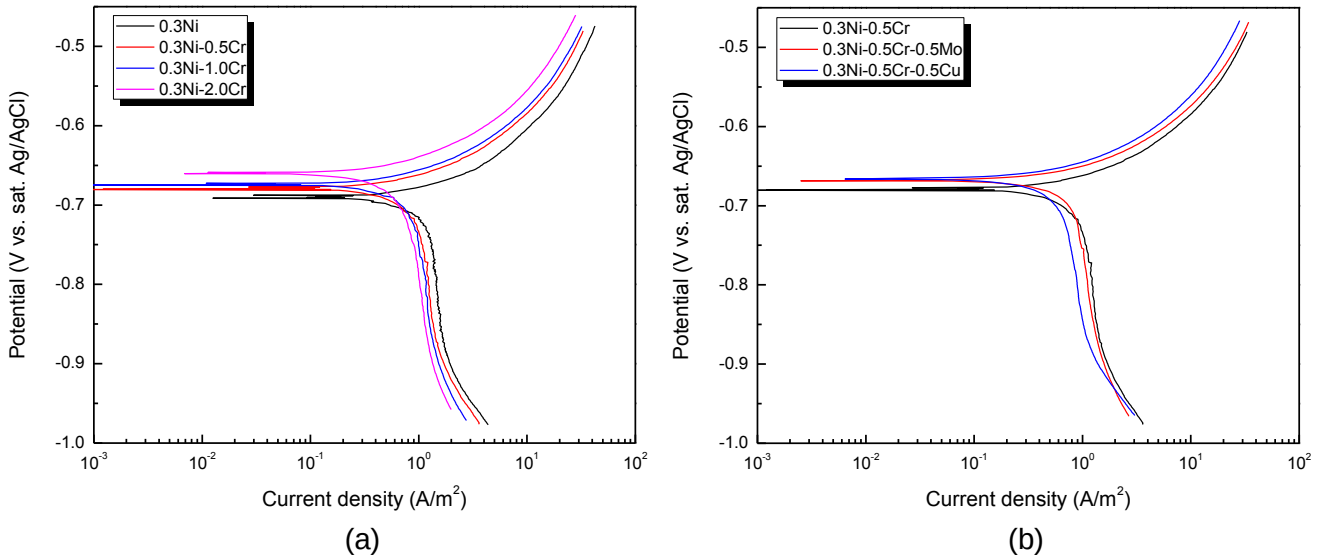

Figure 3: Polarization curves of different carbon steels at pH 4 and 25°C: (a) Cr effect, (b) Mo and Cu effect.

Figure 4 shows the variations in corrosion rate and corrosion potential with time for different carbon steels in 1 wt.% NaCl at pH 4 and 25°C. 0.3Ni-2.0Cr and 0.3Ni-0.5Cr-0.5Cu steels were selected to conduct long-term corrosion tests since those two steels showed the lowest corrosion rate from the short-term LPR measurement. The corrosion rate and the corrosion potential of 0.3Ni steel increased with time, whereas, steels with Cr and Cu showed more or less constant corrosion rate and corrosion potential with time. The fluctuation of corrosion rate was caused by the room temperature change (~ 10°C) during a day. The corrosion rates of steels with Cr and Cu were slightly lower than that of unalloyed steel, and there is no significant difference in the corrosion rate between 0.3Ni-2.0Cr steel and 0.3Ni-0.5Cr-0.5Cu steel at pH 4 and 25°C.

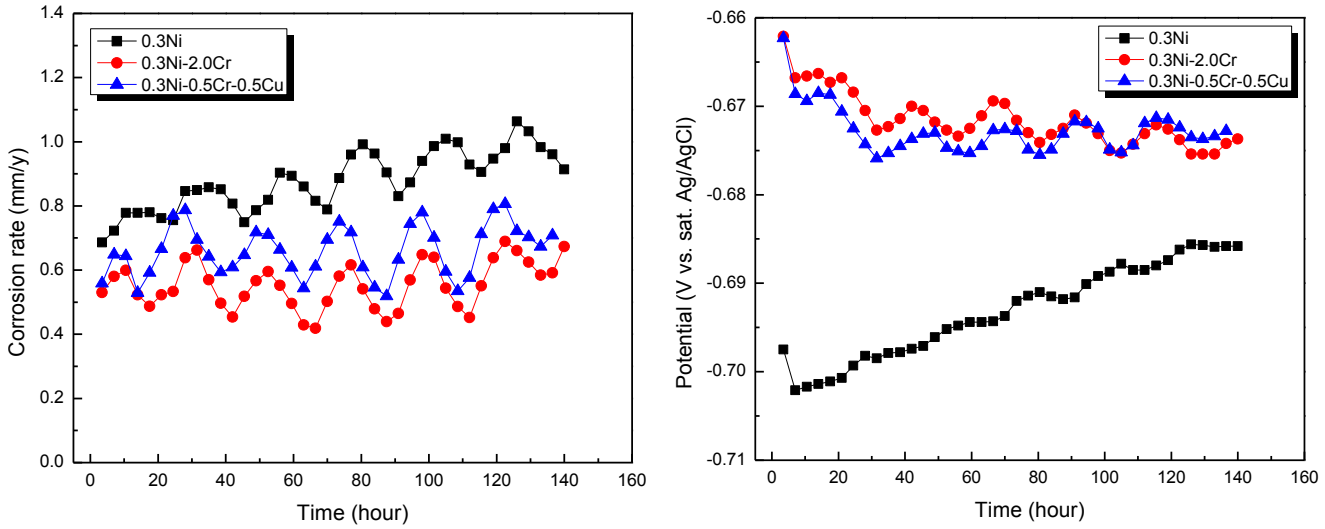

(a) (b)

Figure 4: Variations of (a) corrosion rate and (b) corrosion potential for carbon steels with different alloying elements at pH 4 and 25ºC.

Figure 5 shows the surface and cross-sectional SEM images of the corroded samples after 7 days in 1wt.% NaCl at pH 4 and 25ºC. For all 3 samples, no corrosion products were observed on the surface because of the test condition (low pH and temperature), and it showed mild preferential dissolution of ferrite which left iron carbide (Fe_3C) from the pearlite on the steel.

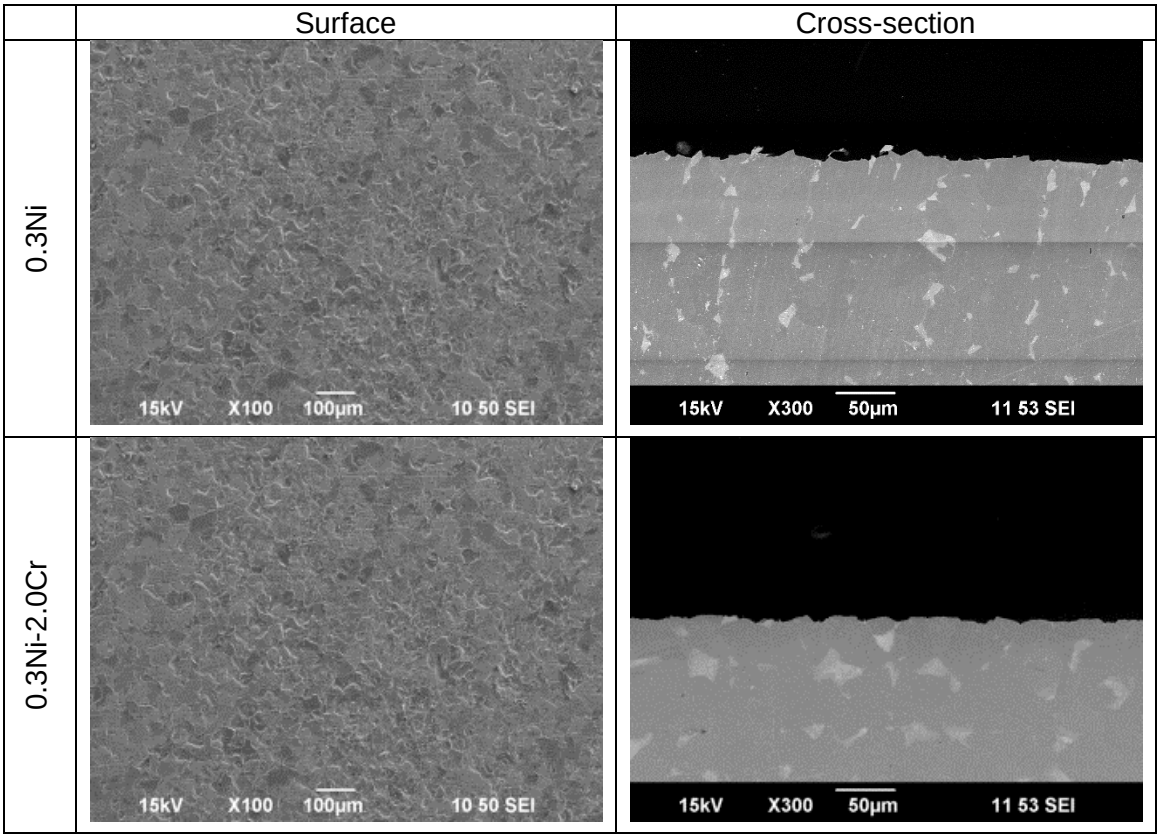

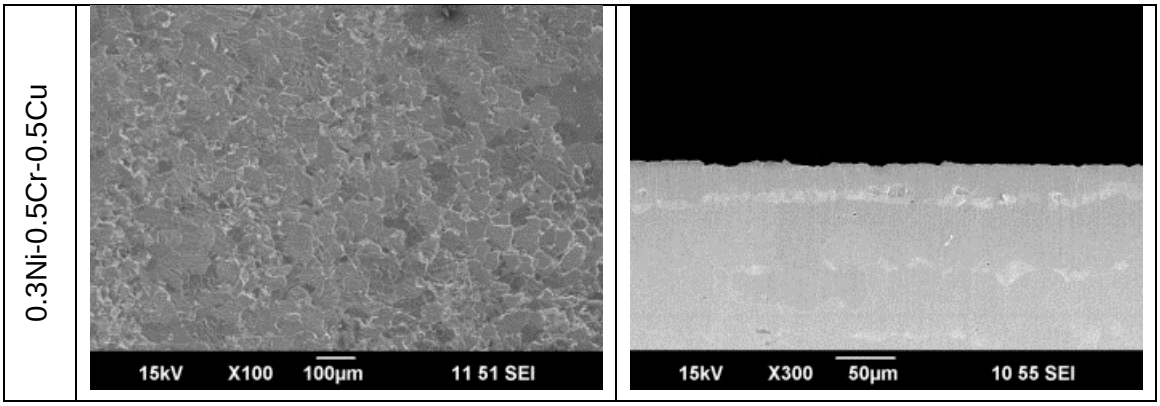

Figure 5: SEM surface and cross-section images of the corroded samples exposed to 1 wt.% NaCl at pH 4 and 25°C.

Experiments at pH 6.6 and 80°C

For these conditions where the formation of protective $FeCO_3$ corrosion product layers was expected, the variations in corrosion rate and corrosion potential with time for different carbon steels in 1 wt.% NaCl at pH 6.6 and 80°C are shown in Figure 6 and Figure 7. In contrast to the corrosion behavior at ambient temperature, the corrosion rate of all steel samples decreased with time and reached to low value (< 0.1 mm/y) at the end of the experiment. In addition, the corrosion potential of all samples increased when the corrosion rate started to decrease. This indicates that protective iron carbonate ($FeCO_3$) layers formed on the steel surface regardless of the alloying elements. The alloying element seemed to affect only the time that it took the corrosion rate to reach the low value.

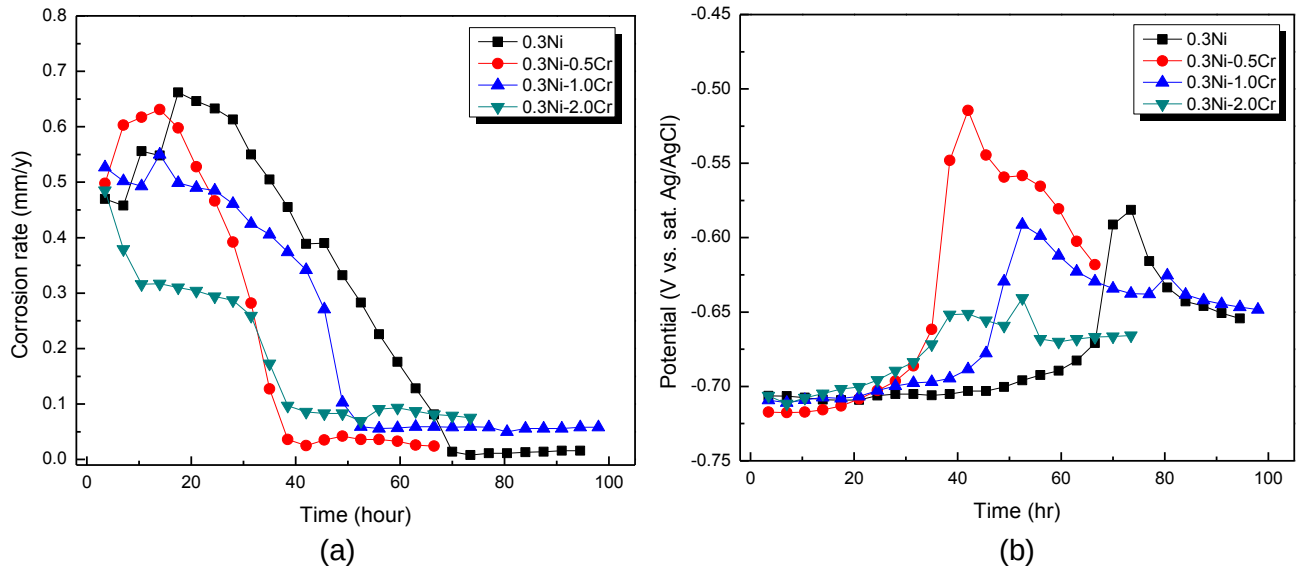

Figure 6: Variations of (a) corrosion rate and (b) corrosion potential for carbon steels with different Cr contents at pH 6.6 and 80°C.

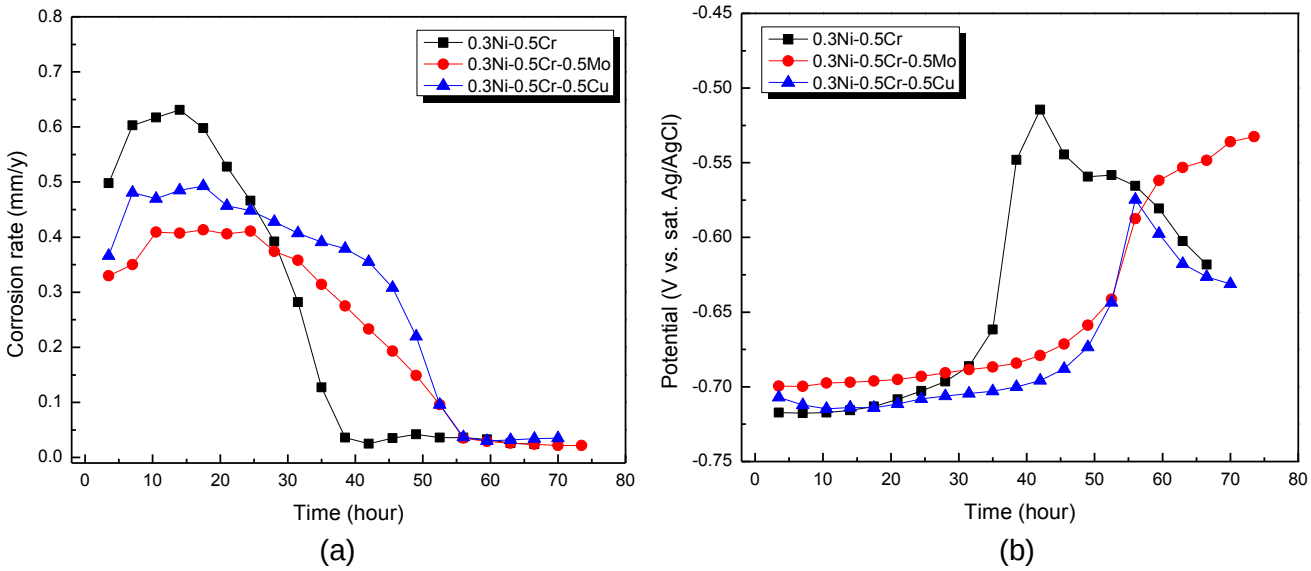

Figure 7: Variations of (a) corrosion rate and (b) corrosion potential for carbon steels with different alloy elements (Mo and Cu) at pH 6.6 and 80ºC.

Figure 8 shows the surface SEM images of the corroded samples at pH 6.6 and 80ºC after 3 days. A typical shape of $FeCO_3$ crystals is observed for all samples. There is no correlation between the size of the corrosion product and the alloying elements, the variation is random. It is interesting to note that for all steel samples, the surface does not appear to be fully covered by corrosion products, even though low corrosion rates were measured as shown in Figure 6 (a) and Figure 7 (a). This is due to a much thinner firmly adherent layer that is not readily seen in these images.

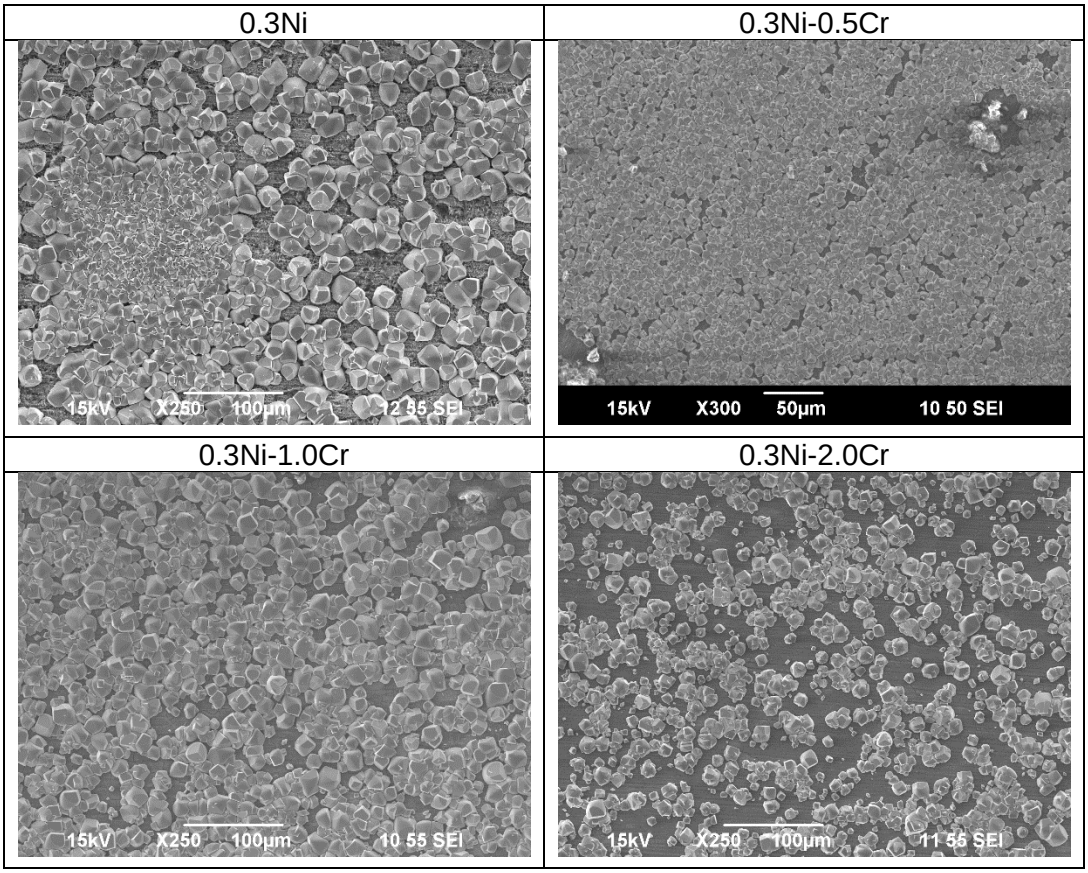

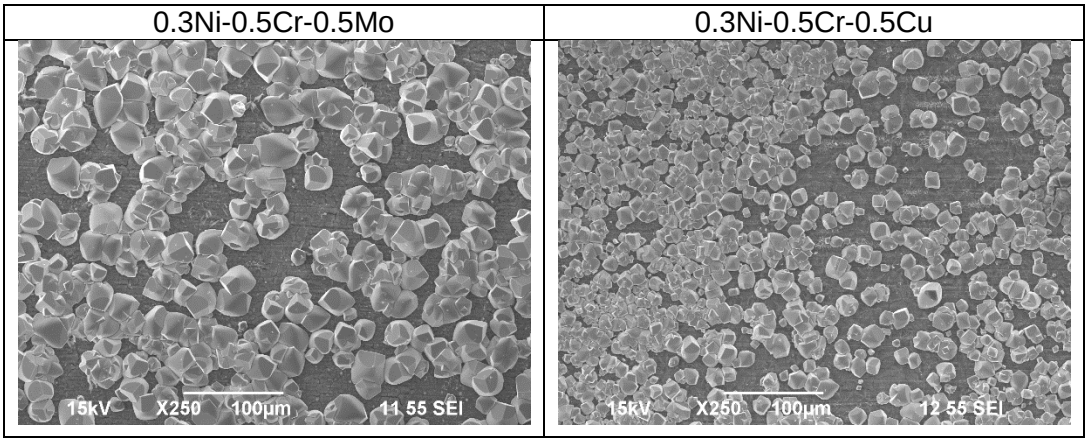

Figure 8: SEM surface images of the corroded samples exposed to 1 wt.% NaCl at pH 6.6 and 80°C.

Figure 9 represents the cross-sectional morphologies of the samples at pH 6.6 and 80°C after 3 days. It can be seen from all samples that it has a "duplex" layer structure; an outer crystal layer and a continuous adherent inner layer, which seems to be the key to corrosion protection. Similar corrosion product morphologies have been observed recently under different experimental conditions in CO_2 environments.[18] According to EDS results, the outer crystal and inner layer are found to be consistent with $FeCO_3$. The Cr-containing samples showed an enrichment of Cr at the inner layer, while no Cr was detected at the outer crystals. From the cross-sectional observations, it is clear that the corrosion protection is provided by the inner well-attached and dense $FeCO_3$ layer, and not by the outer $FeCO_3$ crystals. Moreover, the alloying elements (Cr, Mo and Cu) did not contribute to the formation of a more protective $FeCO_3$ layer at pH 6.6 and 80°C.

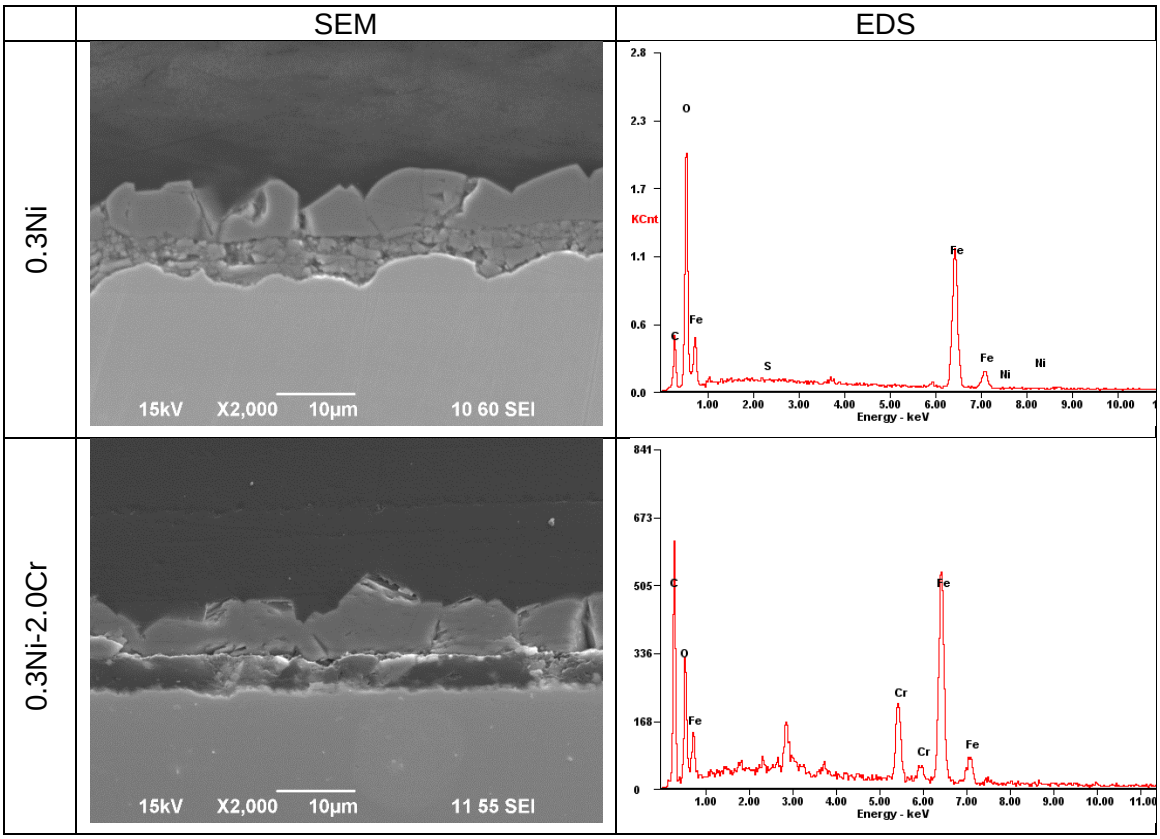

Figure 9: SEM cross-section images and EDS spectra of the corroded samples exposed to 1 wt.% NaCl at pH 6.6 and 80°C.

Experiments at pH 5.9 and 70°C

According to the results shown above, the effect of alloying elements on corrosion behavior was indistinct in both the $FeCO_3$-free condition (pH 4, 25°C) and protective $FeCO_3$-forming condition (pH 6.6, 80°C). In other words, the alloying elements do not play a role neither in the undersaturated nor supersaturated conditions with respect to $FeCO_3$ formation. Thus, to further investigate the effect of alloying elements, long-term corrosion tests were conducted in the near-saturated conditions (at pH 5.9, 70°C), where formation of protective $FeCO_3$ is possible but not certain. This is a condition often referred to as the "grey zone".

The variations in corrosion rate and corrosion potential with time for different carbon steels in 1 wt.% NaCl at pH 5.9 and 70°C are shown in Figure 10 and Figure 11. It is interesting to observe that the corrosion rate of 0.3Ni-1.0Cr and 0.3Ni-2.0Cr steels decreased with time, whereas other steels showed constant high corrosion rate with time. Only 0.3Ni-2.0Cr steel demonstrated a significant decrease in the corrosion rate with time to truly low values, indicating the formation of fully protective corrosion product layer. It can be clearly seen that with increasing Cr content, the final corrosion rate was decreased, whereas no beneficial effect was observed by adding Mo and Cu under this condition. This suggests that the protectiveness of corrosion product strongly depends on the Cr content in the near-saturated "grey zone" condition.

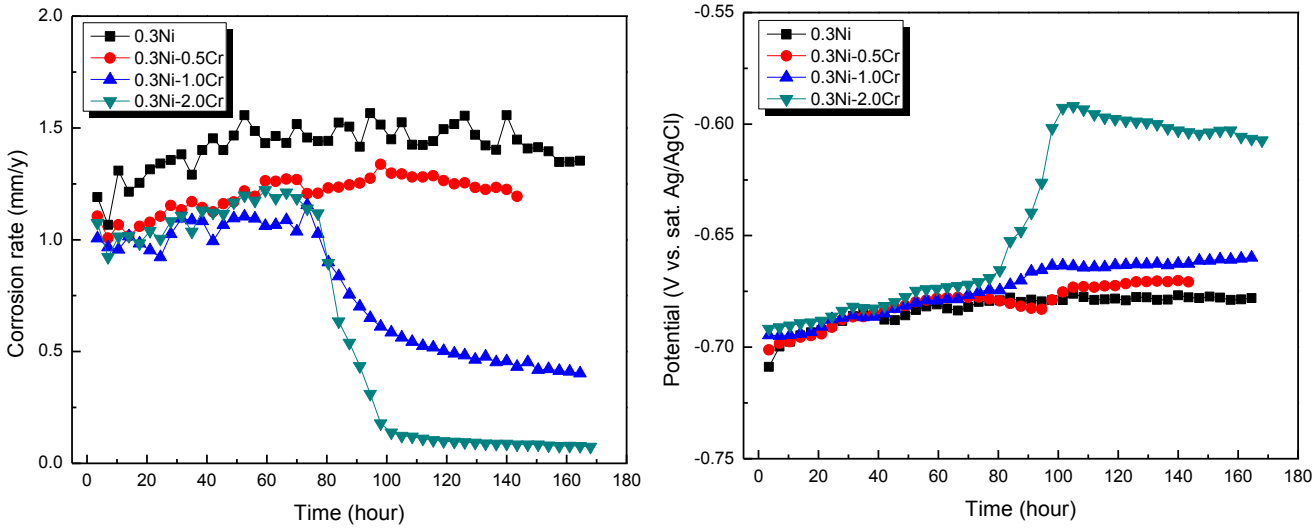

(a) (b)

Figure 10: Variations of (a) corrosion rate and (b) corrosion potential for carbon steels with different Cr contents at pH 5.9 and 70°C.

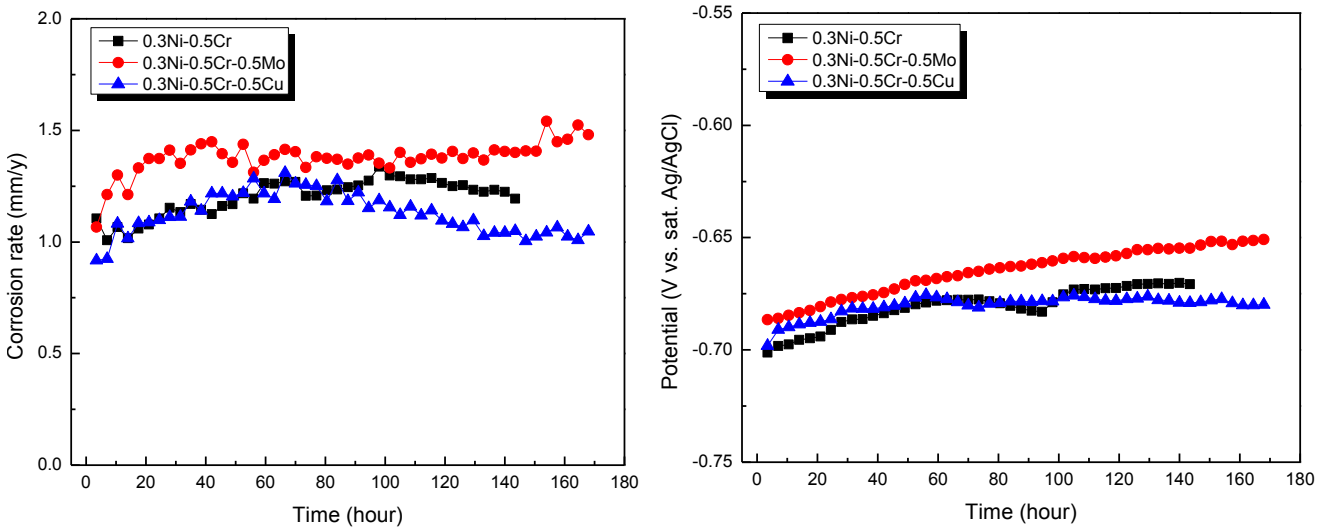

(a) (b)

Figure 11: Variations of (a) corrosion rate and (b) corrosion potential for carbon steels with different alloy elements (Mo and Cu) at pH 5.9 and 70ºC.

Figure 12 shows the surface and cross-sectional SEM images of the corroded samples after 7 days in 1wt.% NaCl at pH 5.9 and 70ºC. Although the surface of 0.3Ni steel was fully covered by crystal shape of $FeCO_3$, the corrosion rate was high as shown in Figure 10 (a). This can be explained by observing the cross-sectional image, which shows no dense inner layer but only the outer $FeCO_3$ crystals. The steels containing Cr showed different morphology compared with 0.3Ni steel, i.e., no $FeCO_3$ crystals were observed, but a dense and adherence layer was formed on the steel surface. The layer became denser and more continuous with increasing Cr content, which provided better corrosion protection. It should be mentioned that the addition of Cu showed no beneficial effect on the formation of protective layer in this condition.

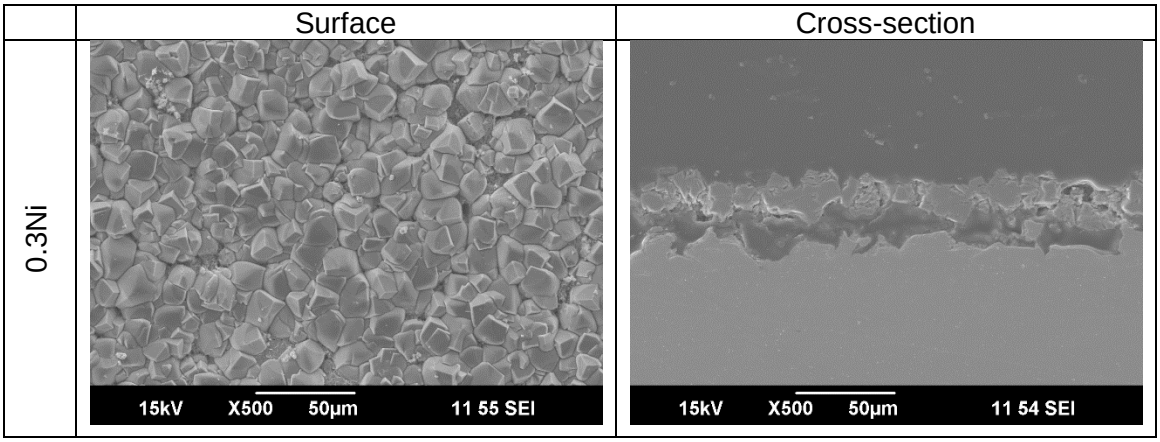

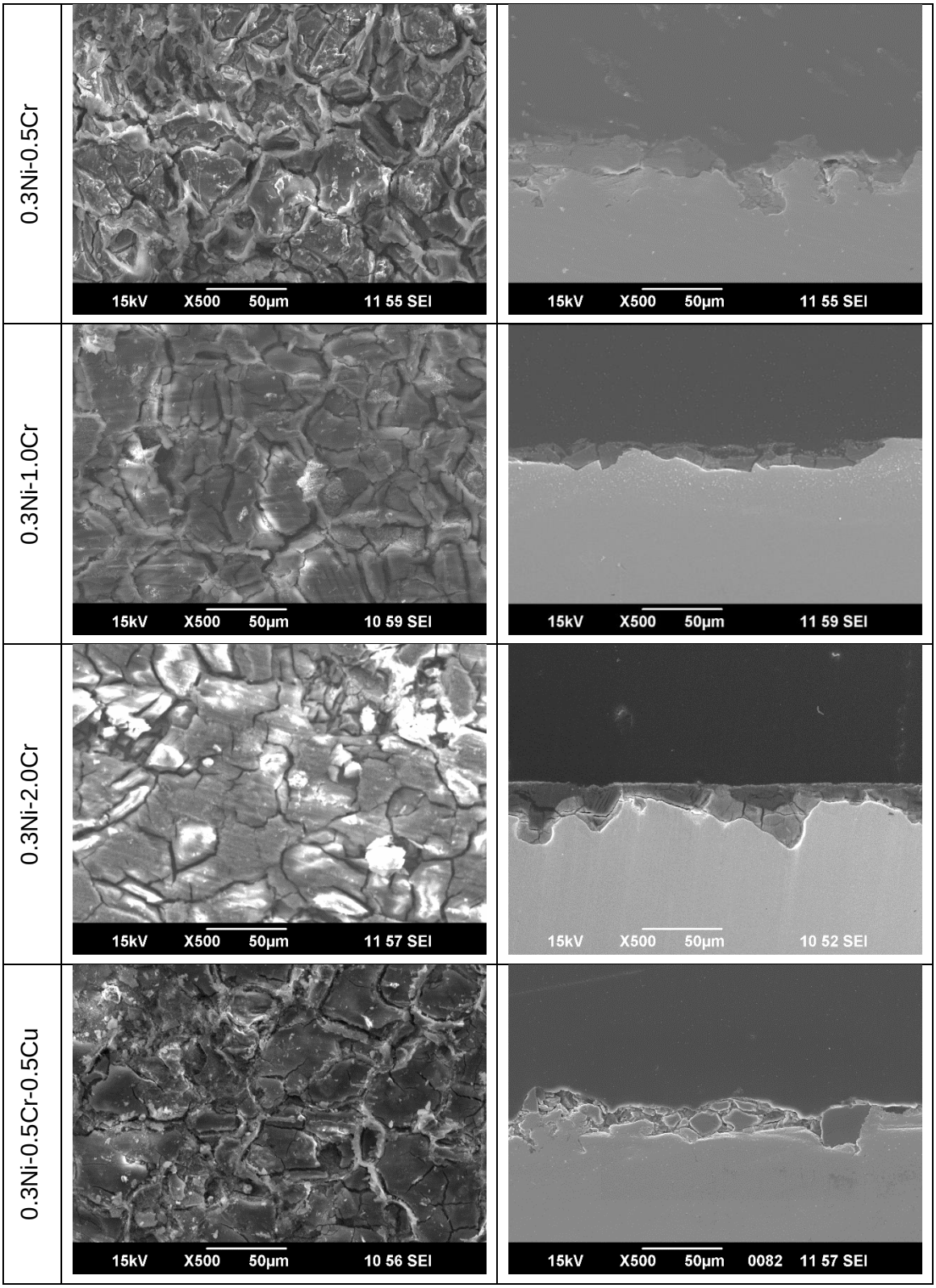

Figure 12: SEM surface and cross-section images of the corroded samples exposed to 1 wt.% NaCl at pH 5.9 and 70ºC.

Details of corrosion scale morphology and composition for 0.3Ni-2.0Cr steel are further examined by cross-sectional SEM and EDS, as shown in Figure 13. The layer consists of two distinct areas with respect to Cr content. It is comprised of Cr-rich area with dark contrast, mainly consisting of Cr and O,

and the other area with relatively light contrast, mainly consisting of $FeCO_3$ (Table 3). The Pd seen in the EDS spectra is from the sputter coated Palladium to avoid any charging during SEM analysis. It has been reported that the addition of Cr results in forming $Cr(OH)_3$ enriched layer within $FeCO_3$.[13] Furthermore, the presence of Cr^{3+} in the solution has a significant effect on the precipitation and growth rate of $FeCO_3$.[19,20] Thus, as shown in Figure 13, the beneficial effect of Cr addition in this condition is confirmed by both forming $Cr(OH)_3$ and promoting the formation of thin but adherent and protective $FeCO_3$ layers.

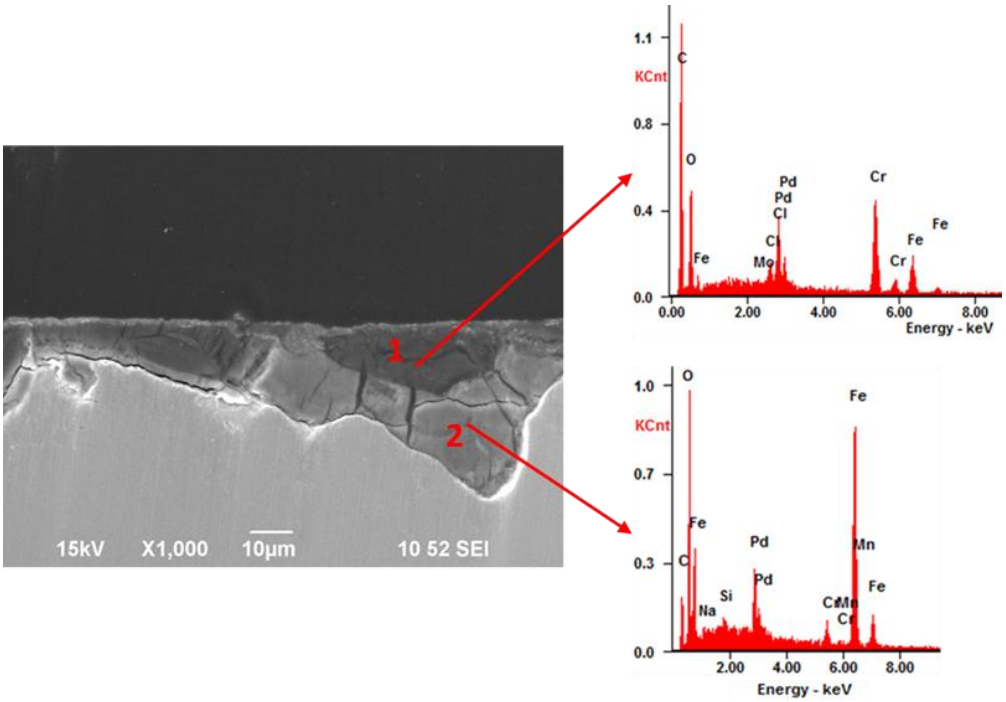

Figure 13: SEM cross-section image and EDS spectra of the corroded sample (0.3Ni-2.0Cr steel) exposed to 1 wt.% NaCl at pH 5.9 and 70ºC.

Table 3
EDS analysis of 0.3Ni-2.0Cr steel exposed to 1 wt.% NaCl at pH 5.9 and 70oC.

	C (At %)	**O** (At %)	**Cr** (At %)	**Fe** (At %)
1	68.03	13.72	9.66	5.24
2	29.43	26.19	1.88	37.94

CONCLUSIONS

The effect of alloying elements (Cr, Mo and Cu) on the corrosion behavior of low carbon steel was investigated in different CO_2 environments. The following conclusions are drawn:

- The addition of Cr and Cu showed a slight positive effect on the corrosion resistance at pH 4.0 and 25ºC – conditions where protective $FeCO_3$ corrosion product layers do not form.
- At pH 6.6 and 80ºC, regardless of the alloying elements, the trend of corrosion rate with time was similar, *i.e.*, the corrosion rate of all specimens decreased with time due to the formation of protective $FeCO_3$ corrosion product layer.
- A beneficial effect of Cr addition was clearly seen at pH 5.9 and 70ºC, conditions where protective $FeCO_3$ corrosion product layers could form, but their protectiveness is not certain – in the so called "grey zone". The steel sample without Cr showed high corrosion rate with time. The presence of Cr promoted the formation of protective $FeCO_3$ layers with Cr enrichment what decreased the corrosion rate significantly.

REFERENCES

1. M. Finšgar, J. Jackson, “Application of Corrosion Inhibitors for Steels in Acidic Media for the Oil and Gas Industry: A Review,” *Corrosion Science* 86 (2014): p. 17.
2. Q. Wu, Z. Zhang, X. Dong, J. Yang, “Corrosion Behavior of Low-Alloy Steel Containing 1% Chromium in CO_2 Environments,” *Corrosion Science* 75 (2013): 400.
3. L.G.S. Gray, B.G. Anderson, M.J. Danysh, P.R. Tremaine, “Effect of pH and Temperature on the Mechanism of Carbon steel Corrosion by Aqueous Carbon Dioxide,” CORROSION 90, paper no. 40 (Houston, TX: NACE, 1990).
4. C. de Waard, U. Lotz, A. Dugstad, “Influence of Liquid Flow Velocity on CO_2 Corrosion: A Semi-Empirical Model,” CORROSION 95, paper no. 254 (Houston, TX: NACE, 1995).
5. S. Nesic, J. Postlethwaite, S. Olsen, “An Electrochemical Model for Prediction of Corrosion of Mild Steel in Aqueous Carbon Dioxide Solutions,” *Corrosion* 52 (1996): p. 280.
6. S. Nesic, “Key Issues Related to Modelling of Internal Corrosion of Oil and Gas Pipelines – A Review,” *Corrosion Science* 49 (2007): p. 4308.
7. W. Li, Y. Xiong, B. Brown, K. E. Kee, S. Nesic, “Measurement of Wall Shear Stress in Multiphase Flow and its Effect on Protective $FeCO_3$ Corrosion Product Layer Removal,” CORROSION 2015, paper no. 5922 (Houston, TX: NACE, 2015).
8. D.A. Lopez, T. Perez, S.N. Simison, “The Influence of Microstructure and Chemical composition of carbon and low alloy steels in CO2 Corrosion: A State-of-the-Art Appraisal,” Materials & Design 24 (2003): p. 561.
9. T. Muraki, T. Hara, K. Nose, H. Asahi, “Effects of Chromium Content up to 5% and Dissolved Oxygen on CO_2 Corrosion,” CORROSION 2002, paper no. 02272 (Houston, TX: NACE, 2002).
10. L. Xu, B. Wang, J. Zhu, W. Li, Z. Zheng, “Effect of Cr Content on the Corrosion Performance of Low-Cr Alloy Steel in a CO_2 Environment,” *Applied Surface Science* 379 (2016): 39.
11. M. Ueda, H. Takabe, “The Formation Behavior of Corrosion Protective Films of Low Cr Bearing Steels in CO_2 Environments,” CORROSION 2001, paper no. 01066 (Houston, TX: NACE, 2001).
12. T. Chen, L. Xu, M. Lu, W. Chang, L. Zhang, “Study on Factors Affecting Low Cr Alloy Steels in a CO_2 Corrosion System,” CORROSION 2011, paper no. 11074 (Houston, TX: NACE, 2011).
13. S. Guo, L. Xu, L. Zhang, W. Chang, M. Lu, “Corrosion of Alloy Steels Containing 2% Chromium in CO_2 Environments,” *Corrosion Science* 63 (2012): 246.
14. S. Hassani, T.N. Vu, N.R. Rosli, S.N. Esmaeely, Y.S. Choi, D. Young, S. Nesic, “Wellbore Integrity and Corrosion of Low Alloy and Stainless Steels in High Pressure CO_2 Geologic Storage Environments: An experimental study,” *International Journal of Greenhouse Gas Control* 23 (2014): 30.
15. J.H. Park, H.S. Seo, K.Y. Kim, S.J. Kim, “The Effect of Cr on the Electrochemical Corrosion of High Mn Steel in a Sweet Environment.” *Journal of The Electrochemical Society* 163 (2016): C791.
16. W. Li, L. Xu, L. Qiao, J. Li, “Effect of Free Cr Content on Corrosion Behavior of 3Cr Steels in a CO_2 Environment,” *Applied Surface Science* 425 (2017): 32.
17. D.V. Edmonds, R.C. Cochrane, “The Effect of Alloying on the Resistance of Carbon Steel for Oilfield Applications to CO_2 Corrosion,” *Materials Research* 8 (2005): 377.
18. W. Li, B. Brown, D. Young, S. Nesic, “Investigation of Pseudo-Passivation of Mild Steel in CO_2 Corrosion,” CORROSION 2013, paper no. 2149 (Houston, TX: NACE, 2013).
19. B. Ingham, M. Ko, N. Laycock, N.M. Kirby, D.E. Williams, “First Stages of Siderite Crystallisation during CO_2 Corrosion of Steel Evaluated Using In Situ Synchrotron Small- and Wide-Angle X-Ray Scattering,” *Faraday Discussions* 180 (2015): 171.
20. M. Ko, B. Ingham, N. Laycock, D.E. Williams, “In Situ Synchrotron X-Ray Diffraction Study of the Effect of Microstructure and Boundary Layer Conditions on CO_2 Corrosion of Pipeline Steels,” *Corrosion Science* 90 (2015): 192.